The Astrophysical Journal Letters, 879:L16 (5pp), 2019 July 1 https://doi.org/10.3847/2041-8213/ab288a

On the Interpretation of *Parker Solar Probe* Turbulent Signals

Sofiane Bourouaine and Jean C. Perez
Department of Aerospace, Physics and Space Science, Florida Institute of Technology, 150 West University Boulevard, Melbourne, FL 32901, USA
sbourouaine@fit.edu
Received 2019 May 17; revised 2019 June 5; accepted 2019 June 9; published 2019 July 2

Abstract

In this Letter we propose a practical methodology to interpret future *Parker Solar Probe* (*PSP*) turbulent time signals even when Taylor's hypothesis is not valid. By extending Kraichnan's sweeping model used in hydrodynamics we derive the Eulerian spacetime correlation function in magnetohydrodynamic (MHD) turbulence. It is shown that in MHD, the temporal decorrelation of small-scale fluctuations arises from a combination of hydrodynamic sweeping induced by large-scale fluid velocity δu_0 and by the Alfvénic propagation along the local magnetic field. The resulting temporal part of the spacetime correlation function is used to determine the field-perpendicular wavenumber range $\Delta k_\perp = [k_{\min}, k_{\max}]$ of the turbulent fluctuations that contribute to the power of a given frequency ω of the time signal measured in the spacecraft frame. Our analysis also shows that the shape of frequency power spectrum $P_{sc}(\omega)$ of the time signal will follow the same power law of the reduced power spectrum $E(k_\perp) \sim k_\perp^{-\alpha}$ in the plasma frame, where α is the spectral index. The proposed framework for the analysis of *PSP* time signals entirely relies on two simple dimensionless parameters that can be empirically obtained from *PSP* measurements, namely, $\epsilon = \delta u_0/\sqrt{2}\,V_\perp$ (where $V_\perp$ is the perpendicular velocity of *PSP* seen in the plasma frame) and the spectral index α.

Key words: magnetohydrodynamics (MHD) – solar wind – turbulence – waves

1. Introduction

The recently launched *Parker Solar Probe* (*PSP*) mission is expected to make in situ measurements of the solar wind plasma from heliocentric distances of about $r \simeq 9.5R_\odot$ (where $R_\odot$ is one solar radius), near the Alfvén critical point, up to distances as high as $r \simeq 200R_\odot$ (Fox et al. 2016). *PSP* will thus become the first mission to explore the solar wind in the region between $r \simeq 9.5\,R_\odot$ and $r \simeq 60R_\odot$. Beyond these distances, Taylor's Hypothesis (TH; Taylor 1938) is valid as the solar wind velocity U_{sw} is much higher than the propagation and turbulent velocities of the fluctuations. This so-called frozen-in-flow TH has been widely used to relate the power spectrum measured in the spacecraft frame to the reduced power spectrum of the turbulence expected in the plasma frame using the standard relation between the frequency of the signal, ω, and the wavenumber, k, of the turbulent structures in the plasma frame $\omega \simeq \boldsymbol{k}\cdot\boldsymbol{U}_{SW}$ (see e.g., Horbury et al. 2008; Alexandrova et al. 2010; Bourouaine et al. 2012; Bourouaine & Chandran 2013; Chen et al. 2014).

As *PSP* will explore the plasma of the inner heliosphere, there has been an increased and renewed interest in revisiting the validity of the TH in the solar wind. Recently, Bourouaine & Perez (2018, hereafter BP18), investigated the validity of TH near $r \simeq 10R_\odot$ using numerical simulations of reflection-driven magnetohydrodynamic (MHD) turbulence. The authors found that the Eulerian spacetime structure of the turbulence allows for the interpretation of time signals even when TH is not applicable, which is largely consistent with similar works (Matthaeus et al. 2010, 2016; Servidio et al. 2011; Narita et al. 2013; Weygand et al. 2013; Klein et al. 2014, 2015; Narita 2017), but with a number of important differences. For instance, BP18 found that the Eulerian decorrelation in simulations is consistent with spectral broadening associated with pure hydrodynamic sweeping by the large-scale eddies, combined with a Doppler shift associated with Alfvénic propagation along the background magnetic field. BP18, in agreement with Narita (2017), also found that the temporal dependency of the Eulerian correlation is more consistent with a Gaussian decay than exponential decay found by Servidio et al. (2011) and Lugones et al. (2016). Another important difference with previous works is that BP18 found that the decorrelation is the same for oppositely propagating fluctuations even when the turbulence is imbalanced (non-zero cross-helicity).

In this Letter, we propose a model for the Eulerian spacetime correlation function in the context of MHD turbulence based on Kraichnan's sweeping hypothesis (KSH) in hydrodynamics (Kraichnan 1964). We also show that the proposed analytical model can be used to interpret *PSP* time signals, solely relying on two empirical parameters that can be easily measured from observations.

2. Eulerian Spacetime Correlation

We assume statistically homogeneous and stationary magnetized MHD turbulence and describe the evolution of fluctuations in terms of the Elssaser variables $\boldsymbol{z}^\pm = \delta\boldsymbol{u} \pm \delta\boldsymbol{v}_A$

$$\frac{\partial \boldsymbol{z}^\pm}{\partial t} \mp \boldsymbol{v}_A\cdot\boldsymbol{\nabla}\boldsymbol{z}^\pm = -\boldsymbol{z}^\mp\cdot\boldsymbol{\nabla}\boldsymbol{z}^\pm - \nabla p, \tag{1}$$

where $\boldsymbol{v}_A = \boldsymbol{B}_0/(4\pi\rho)$ is the background Alfvén velocity, ρ is the density of the fluid, $\delta\boldsymbol{v}_A(\boldsymbol{x}, t)$, and $\delta\boldsymbol{u}(\boldsymbol{x}, t)$ are the fluctuating Alfvén and fluid velocity, respectively. We define the Eulerian spacetime correlation function $C^\pm(\boldsymbol{x}, \tau)$ for $\boldsymbol{z}^\pm$ as

$$C^\pm(\boldsymbol{x}, \tau) = \langle \boldsymbol{z}^\pm(\boldsymbol{x}_0, t_0)\cdot\boldsymbol{z}^\pm(\boldsymbol{x}_0+\boldsymbol{x}, t_0+\tau)\rangle, \tag{2}$$

where $\langle\cdots\rangle$ denotes the ensemble average over many turbulence realizations. In the homogeneous and stationary state, the correlation only depends on the spacetime lags $\boldsymbol{x}$ and τ, and its

space Fourier transform becomes

$$h^{\pm}(\boldsymbol{k}, \tau) = \frac{1}{(2\pi)^3} \int C^{\pm}(\boldsymbol{x}, \tau) e^{-i\boldsymbol{k}\cdot\boldsymbol{x}} d^3x, \tag{3}$$

which is also known as the two-time energy spectrum.

We model the Eulerian correlation by extending the KSH, i.e., that the spacetime structure of small-scales eddies in the Eulerian description is dominated by random sweeping by large-scale fluctuations. In MHD, the random sweeping of small-scale eddies by large-scale ones can occur either from the large-scale bulk flow, which we call hydrodynamic sweeping, as well as the wave propagation of the $\boldsymbol{z}^{\pm}$ along and against the local magnetic field that results from the perturbation of the background field by the large-scale eddies, which we call Alfvén-wave sweeping. This can be made evident by replacing the advecting fields $\boldsymbol{z}^{\mp} = \delta\boldsymbol{u} \mp \delta\boldsymbol{v}_{\rm A}$ in Equation (1) to obtain

$$\frac{\partial \boldsymbol{z}^{\pm}}{\partial t} + (\delta\boldsymbol{u} \mp \boldsymbol{V}_{\rm A}) \cdot \boldsymbol{\nabla} \boldsymbol{z}^{\pm} = 0, \tag{4}$$

where $\boldsymbol{V}_{\rm A} = \boldsymbol{v}_{\rm A} + \delta\boldsymbol{v}_{\rm A}$ is the *local* Alfvén velocity. The pressure has been ignored as its role is only to keep the fluctuations incompressible. In Equation (4) the Elsässer fields $\boldsymbol{z}^{\pm}$ undergo random advection both by the flow $\delta\boldsymbol{u}$ and the local Alfvén velocity $\boldsymbol{V}_{\rm A}$. We extend KSH in MHD by replacing the advecting variables $\delta\boldsymbol{u}$ and $\delta\boldsymbol{v}_{\rm A}$ with zero-mean random fields $\delta\boldsymbol{u}'$ and $\delta\boldsymbol{v}'_{\rm A}$ with prescribed statistics, which we take to be Gaussian for simplicity. Hereafter, primed variables indicate the field is a random variable with prescribed statistics. We further assume that all fluctuating fields, $\boldsymbol{z}^{\pm}$, $\delta\boldsymbol{u}'$ and $\delta\boldsymbol{v}'_{\rm A}$, are perpendicular to the local mean magnetic field, namely, the direction of $\boldsymbol{V}'_{\rm A} \equiv \boldsymbol{v}_{\rm A} + \delta\boldsymbol{v}'_{\rm A}$. The space Fourier transform of $\boldsymbol{z}^{\pm}$ then follows the linear equation

$$\frac{\partial \tilde{\boldsymbol{z}}^{\pm}}{\partial t} + i(\boldsymbol{k}_{\perp} \cdot \delta\boldsymbol{u}' \mp k_{\parallel} V'_{\rm A}) \tilde{\boldsymbol{z}}^{\pm} = 0, \tag{5}$$

where $\tilde{\boldsymbol{z}}^{\pm} = \tilde{\boldsymbol{z}}^{\pm}(\boldsymbol{k}, t)$ is the space Fourier transform of $\boldsymbol{z}^{\pm}(\boldsymbol{x}, t)$. It is important to notice that the parallel wavenumber $k_{\parallel}$ in this equation represents the wave-vector with respect to the local magnetic field (along $\boldsymbol{V}'_{\rm A}$) and not along the background magnetic field (along $\boldsymbol{B}_0$). Equation (5) is a stochastic linear equation whose solution is

$$\tilde{\boldsymbol{z}}^{\pm}(\boldsymbol{k}, t) = \tilde{\boldsymbol{z}}^{\pm}(\boldsymbol{k}, 0) e^{\pm i k_{\parallel} V'_{\rm A} t} e^{-i\boldsymbol{k}_{\perp}\cdot\delta\boldsymbol{u}' t}. \tag{6}$$

An important additional simplification follows for strongly magnetized turbulence, $\delta v'_{\rm A} \ll v_{\rm A}$, in which case $V'_{\rm A} = v_{\rm A}(1 + \delta v'^2_{\rm A}/v^2_{\rm A})^{1/2} \approx v_{\rm A}$, and therefore

$$\tilde{\boldsymbol{z}}^{\pm}(\boldsymbol{k}, t) = \tilde{\boldsymbol{z}}^{\pm}(\boldsymbol{k}, 0) e^{\pm i k_{\parallel} v_{\rm A} t} e^{-i\boldsymbol{k}_{\perp}\cdot\delta\boldsymbol{u}' t}. \tag{7}$$

This model presents a number of significant advantages over previous approaches based on the KSH (Matthaeus et al. 2010; Servidio et al. 2011; Narita et al. 2013; Weygand et al. 2013; Narita 2017). The first is that because the random variation of $\delta\boldsymbol{v}'_{\rm A}$ does not affect the magnitude of the local Alfvén velocity $\boldsymbol{V}'_{\rm A}$, to first order in $\delta v'_{\rm A}/v_{\rm A}$, the Alfvénic sweeping is not random. The second advantage is that in the solution provided by Equation (7) the parallel and perpendicular components of the wave-vector $\boldsymbol{k}$ are defined with respect to the direction of the local, fluctuating magnetic field and not with respect to the constant background field. Lastly, as we will see in more detail later, the spectral broadening associated with sweeping solely arises from random advection by the velocity of large-scale eddies, and therefore affects both Elsässer components $\boldsymbol{z}^{\pm}$ equally.

Assuming that $\tilde{\boldsymbol{z}}^{\pm}$ and $\delta\boldsymbol{u}'$ are statistically independent at $t = 0$, it is straightforward to demonstrate that the two-time power spectrum $h^{\pm}(\boldsymbol{k}, \tau)$ defined by Equation (3) becomes

$$\begin{aligned} h^{\pm}(\boldsymbol{k}, \tau) &= \langle \tilde{\boldsymbol{z}}^{\pm}(\boldsymbol{k}, t) \cdot \tilde{\boldsymbol{z}}^{\pm}(-\boldsymbol{k}, t + \tau) \rangle, \\ &= h_0^{\pm}(\boldsymbol{k}) e^{\mp i k_{\parallel} v_{\rm A} \tau} \langle e^{i\boldsymbol{k}_{\perp}\cdot\delta\boldsymbol{u}'\tau} \rangle, \end{aligned} \tag{8}$$

where $h_0^{\pm}(\boldsymbol{k}) = h^{\pm}(\boldsymbol{k}, 0)$ is the three-dimensional power spectrum, or the one-time ($\tau = 0$) energy spectrum. Equation (8) indicates that the temporal decorrelation is the result of pure hydrodynamic sweeping, Doppler-shifted by Alfvénic propagation along the local magnetic field. For simplicity we assume that the component $\delta u'_n = \hat{\boldsymbol{n}} \cdot \delta\hat{\boldsymbol{u}}'$ along any direction $\hat{\boldsymbol{n}}$ is described by a Gaussian probability density $g(\delta\hat{u}'_n)$ where

$$g(x) = \frac{1}{\sqrt{2\pi}} e^{-\frac{1}{2}x^2}, \tag{9}$$

$\delta\hat{u}'_n \equiv \sqrt{2}\,\delta u'_n/\delta u_0$, and $\delta u_0 = \sqrt{\langle |\delta\boldsymbol{u}'|^2 \rangle}$ is the root mean square value of $\delta\boldsymbol{u}'$. Equation (8) then becomes

$$h^{\pm}(\boldsymbol{k}, \tau) = h_0^{\pm}(\boldsymbol{k}) \Gamma^{\pm}(\boldsymbol{k}, \tau), \tag{10}$$

where

$$\Gamma^{\pm}(\boldsymbol{k}, \tau) \equiv e^{\mp i k_{\parallel} v_{\rm A} \tau} e^{-\frac{1}{4}(\delta u_0 k_{\perp} \tau)^2}. \tag{11}$$

The function $\Gamma^{\pm}(\boldsymbol{k}, \tau)$ describes the temporal dependency of the two-time spectrum $h^{\pm}(\boldsymbol{k}, \tau)$ and determines the scale-dependent Eulerian decorrelation time of the turbulence.

The choice of a Gaussian probability density is made for analytical convenience. However, the results that we present here have general validity for any other probability density, including one empirically obtained from spacecraft data.

3. Frequency Spectrum in the Spacecraft Frame

The frozen-in-flow TH is valid in solar wind data when the speed of the the spacecraft seen in the plasma frame $V_{\rm sc} = |\boldsymbol{V}_{\rm sc}|$ is much higher than the propagation velocity $v_{\rm ph}$ and velocity amplitudes δu_0 of the turbulent fluctuations, and thus the frequency ω of the signal can be related to turbulent fluctuation scale $1/k$ as $\omega \simeq |\boldsymbol{k} \cdot \boldsymbol{V}_{\rm sc}|$. However, in our analysis we will show that there are other cases in which we can still connect ω to k even if $V_{\rm sc} \sim v_{\rm ph}$. The key quantity that determines this criterion is the decorrelation function $\Gamma^{\pm}(\boldsymbol{k}, \tau)$ defined in Equation (11).

Following Horbury et al. (2008) and Bourouaine & Chandran (2013), the power spectrum from single-point measurements in the spacecraft frame $P^{\pm}_{\rm sc}(\omega)$ is related to the three-dimensional power measured in the plasma frame by expression

$$P^{\pm}_{\rm sc}(\omega) = \frac{1}{2\pi} \int h^{\pm}(\boldsymbol{k}, \tau) e^{i(\omega + \boldsymbol{k}\cdot\boldsymbol{V}_{\rm sc})\tau} d\tau d^3k, \tag{12}$$

which upon substitution of $h^{\pm}(\boldsymbol{k}, \tau)$ from Equation (10) gives

$$P_{\rm sc}^{\pm}(\omega) = \frac{1}{2\pi}\int h_0^{\pm}(\boldsymbol{k})\Gamma^{\pm}(\boldsymbol{k}, \tau)e^{i(\omega+\boldsymbol{k}\cdot\boldsymbol{V}_{\rm sc})\tau}d\tau d^3k, \\ = \int h_0^{\pm}(\boldsymbol{k})\tilde{\Gamma}^{\pm}(\boldsymbol{k}, \omega)d^3k, \quad (13)$$

where

$$\tilde{\Gamma}^{\pm}(\boldsymbol{k}, \omega) = \frac{1}{2\sqrt{\pi}\gamma}e^{-\frac{(\omega\mp k_{\parallel}v_{\rm A}+\boldsymbol{k}\cdot\boldsymbol{V}_{\rm sc})^2}{4\gamma^2}}. \quad (14)$$

Here $\gamma = k_{\perp}\delta u_0/2$ represents the spectral broadening around the Doppler-shifted frequency $\boldsymbol{k}\cdot\boldsymbol{V}_{\rm sc}$, the same for both $z^{\pm}$.

Intuitively, the TH relies on the assumption that the spacecraft is moving through the plasma (or the plasma passing by the spacecraft) so fast that the turbulence is "frozen-in," or simply, the turbulence does not have sufficient time to evolve during the observation time. The decorrelation function contains two independent characteristic velocities, the Alfvén speed $v_{\rm A}$, and the velocity rms δu_0, associated with Alfvén-wave advection and random hydrodynamic sweeping. One can parameterize the decorrelation function with $\epsilon \equiv \delta u_0/\sqrt{2}V_{\rm sc}$ by normalizing all velocities to $V_{\rm sc}$ and obtain

$$\tilde{\Gamma}_{\epsilon}^{\pm}(\boldsymbol{k}, \omega) = \frac{1}{\epsilon k_{\perp}V_{\rm sc}}g\left(\frac{\omega\mp k_{\parallel}v_{\rm A}+\boldsymbol{k}\cdot\boldsymbol{V}_{\rm sc}}{\epsilon k_{\perp}V_{\rm sc}}\right), \quad (15)$$

which upon substitution in Equation (13) leads to

$$P_{\rm sc}^{\pm}(\omega) = \int h_0^{\pm}(\boldsymbol{k})\tilde{\Gamma}_{\epsilon}^{\pm}(\boldsymbol{k}, \omega)d^3k. \quad (16)$$

In the limit $\epsilon \to 0$ one obtains

$$\lim_{\epsilon\to 0}\int h_0^{\pm}(\boldsymbol{k})\tilde{\Gamma}_{\epsilon}^{\pm}(\boldsymbol{k}, \omega) = \int h_0^{\pm}(\boldsymbol{k})\delta(\omega\mp k_{\parallel}v_{\rm A}+\boldsymbol{k}\cdot\boldsymbol{V}_{\rm sc}), \quad (17)$$

which for existing solar wind observations $\boldsymbol{V}_{\rm sc} \simeq -\boldsymbol{U}_{\rm SW}$, with $U_{\rm SW} \gg v_{\rm A}$ one recovers the commonly used TH condition

$$P_{\rm sc}^{\pm}(\omega) = \int h_0^{\pm}(\boldsymbol{k})\delta(\omega-\boldsymbol{k}\cdot\boldsymbol{U}_{\rm SW}). \quad (18)$$

In this sense, when either one of the two conditions $\epsilon \ll 1$ and $v_{\rm A} \ll V_{\rm sc}$ no longer hold, Equation (16) should be used in lieu of the TH. One should also note that the TH given by Equation (18) also holds when $v_{\rm A} \sim V_{\rm sc}$ provided the turbulence is strongly anisotropic (i.e., $k_{\parallel} \ll k_{\perp}$).

It is worth mentioning that the resulting model for $\tilde{\Gamma}_{\epsilon}^{\pm}(\boldsymbol{k}, \omega)$ only relies on the validity of the KSH, and it is not specific to a turbulence model. Equation (16) allows us in general to relate temporal signals in the spacecraft frame to the spatial properties of the turbulence in the plasma frame, and reduce in the proper limits to the TH. In this sense, as we show in this Letter, these equations allow us to analyze spacecraft signals when the TH is not valid, with the only requirement that the KSH holds. In the following we proceed to explore the usefulness of the more general Equation (16) in the analysis of solar wind observations, with a focus on the upcoming measurements from the *PSP* mission.

Let us define the reduced perpendicular power spectrum $E^{\pm}(k_{\perp}) = 2\pi\int h_0^{\pm}(k_{\perp}, k_{\parallel})k_{\perp}dk_{\parallel}$, and make the following assumptions: (1) the three-dimensional power spectrum is nearly isotropic in the perpendicular plane, (2) the spacecraft velocity in the Sun's frame, $\boldsymbol{V}_{\perp}$, is nearly perpendicular to the magnetic field, and (3) the power spectrum is highly anisotropic, that is, nearly zero for $k_{\parallel} \ll k_{\perp}$. Then Equation (16) becomes

$$P_{\rm sc}^{\pm}(\omega) = \int_0^{\infty} E_{\rm sc}^{\pm}(k_{\perp}, \omega)dk_{\perp}, \quad (19)$$

where

$$E_{\rm sc}^{\pm}(k_{\perp}, \omega) = \frac{1}{k_{\perp}V_{\perp}}E^{\pm}(k_{\perp})\bar{g}_{\epsilon}(\omega/k_{\perp}V_{\perp}) \quad (20)$$

is the spectral density describing the energy distribution among frequencies and perpendicular wavenumber in the spacecraft frame, and the function

$$\bar{g}_{\epsilon}(x) = \frac{2}{\pi}\int_0^{\pi}\frac{1}{\epsilon}g\left(\frac{x+\cos\phi}{\epsilon}\right)d\phi, \quad (21)$$

is the average of $\tilde{\Gamma}_{\epsilon}^{\pm}(\boldsymbol{k}, \omega)$ over the angle ϕ between $\boldsymbol{k}_{\perp}$ and $\boldsymbol{V}_{\perp}$. An additional factor of two has been added to include the contribution to $P_{\rm sc}(\omega)$ from negative frequencies, so we can assume $\omega \geqslant 0$ hereafter. Equations (19) and (20) will form the basis of our proposed methodology.

A few important aspects of the function $\bar{g}_{\epsilon}(x)$ are worth emphasizing: (1) its integral from $x = 0$ to ∞ is equal to one, (2) it is the same for both $E^{\pm}$ energy spectra, and (3) it is smooth for finite ϵ but becomes singular at $x = 1$ in the limit $\epsilon \to 0$. This last property leads to a spectral density highly localized along $\omega = k_{\perp}V_{\perp}$ corresponding to the frozen-in-flow TH, which means that the energy in a small frequency band $d\omega$ around ω entirely arises from fluctuations with wavenumbers in the range $dk_{\perp}$ around $k_{\perp}$, with $k_{\perp} = \omega/V_{\perp}$.

For finite ϵ, the function $\bar{g}_{\epsilon}(x)$ broadens around $x \simeq 1$ and as a result, the energy in the frequency range $d\omega$ around ω results from a broader range of wavenumbers, and therefore a one-to-one association between frequency and wavenumber no longer seems possible. In fact, Equation (19) shows that the fluctuation energy in the range $d\omega$ around ω results from a non-trivial integral over a broad range of wavenumbers weighted by $\bar{g}_{\epsilon}(\omega/k_{\perp}V_{\perp})$.

Let us now determine the power spectrum $P_{\rm sc}(\omega)$ when the spatial power spectrum in the plasma frame follows a power law of the form $E(k_{\perp}) = Ck_{\perp}^{-\alpha}$. Note that we no longer distinguish between $E^{\pm}$ as the following analysis is identical for both spectra. After changing the $k_{\perp}$ integration in terms of the new variable $x = \omega/k_{\perp}V_{\perp}$ Equation (19) becomes

$$P_{\rm sc}(\omega) = \frac{C}{V_{\perp}}\left(\frac{\omega}{V_{\perp}}\right)^{-\alpha}\int_0^{\infty} f_{\epsilon}(\alpha, x)dx, \quad (22)$$

where

$$f_{\epsilon}(\alpha, x) \equiv x^{\alpha-1}\bar{g}_{\epsilon}(x). \quad (23)$$

One must note that (22) is valid if the power law for $E(k_{\perp})$ extends from $k_{\perp} = 0$ to ∞. From this result we infer the following conclusions: (1) $P_{\rm sc}(\omega)$ is also a power law with the same spectral index of the spectrum $E(k_{\perp})$, which is consistent with the findings of Narita (2017) and Bourouaine & Perez (2018); (2) the overall frequency power spectrum is scaled, compared with the case when the TH is valid, by a factor that solely depends on the distribution of large-scale eddies and the spectral index α.

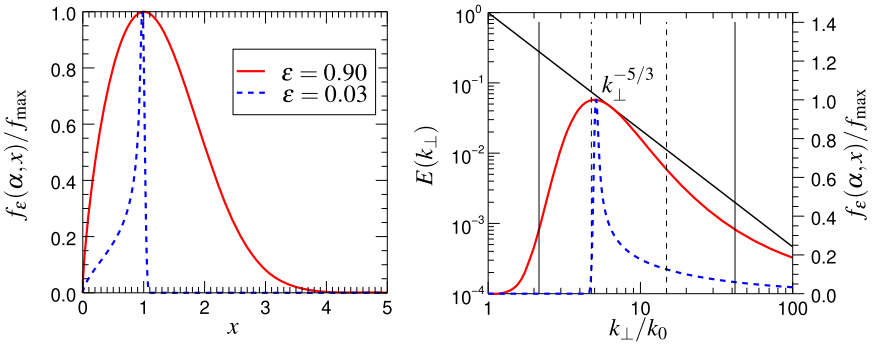

Figure 1. Left panel: function $f(x)$ vs. x for $\epsilon = 0.9$ close to the Sun (solid red curve) and $\epsilon = 0.03$ near 1 au (dashed blue curve). $f(x)$ is normalized to its local maximum $f_{\max}$. Right panel: hypothetical power-law energy spectrum $E(k_\perp) \propto k_\perp^{-\alpha}$ (left vertical axis) and f_ϵ vs. $k_\perp$ for the same values of ϵ.

Equation (22) relating the power spectrum $P_{\rm sc}^{\pm}(\omega)$ in the spacecraft frame to the reduced energy spectrum can be used to define the range of wavenumbers $\Delta k_\perp = [k_{\min}, k_{\max}]$ that provide most of the energy at a given frequency ω. The mapping between a given frequency and the range of wavenumbers providing most of its energy, $\omega \rightarrow \Delta k_\perp$, solely depends on the function $f_\epsilon(\alpha, x)$, determined from parameters ϵ and α, whose values can be obtained from spacecraft observations.

For a fixed set of values ϵ, α, let us define $x_{\min}$ and $x_{\max}$ so that

$$\int_{x_{\min}}^{x_{\max}} f_\epsilon(\alpha, x)dx = \eta \int_0^{\infty} f_\epsilon(\alpha, x)dx \qquad (24)$$

where η is a dimensionless number smaller than one, representing the desired fraction of the total energy contained between $x_{\min}$ and $x_{\max}$. For instance, one can choose $\eta \gtrsim 0.9$ to capture 90% of the total energy. We can then use $x_{\min}$ and $x_{\max}$ to determine the wavenumber range $\Delta k_\perp = [k_{\min}, k_{\max}]$ with the largest contribution to a given frequency ω, as $k_{\min} = \omega/x_{\max} V_\perp$ and $k_{\max} = \omega/x_{\min} V_\perp$, providing most of the power $P_{\rm sc}(\omega)$ at frequency ω.

In the next section we will estimate the frequency-dependent broadening $\Delta k_\perp$ for two different sets of ϵ, α that are representative of the regions that the *PSP* spacecraft is expected to explore.

4. Application to *PSP* Data

At *PSP*'s smallest perihelion, approximately at $9.86 R_\odot$, the spacecraft velocity in the Sun's frame will be approximately $V_\perp \sim 200$ km s^{-1} and nearly perpendicular to the nearly radial magnetic field. In the plasma frame, the spacecraft velocity is $\boldsymbol{V}_{\rm sc} = \boldsymbol{V}_\perp - \boldsymbol{U}_{\rm SW}$, where $\boldsymbol{U}_{\rm SW}$ is the radial solar wind velocity. *PSP*'s perihelion occurs near the Alfvén critical point where $U_{\rm SW} \sim v_{\rm A}$, therefore, based on our strong anisotropy assumption $\boldsymbol{k} \cdot \boldsymbol{V}_{\rm sc} \simeq \boldsymbol{k}_\perp \cdot \boldsymbol{V}_\perp$. We assume that the rms of velocity fluctuations at this heliocentric radius is $\delta u_0 \simeq 250$ km s^{-1}, which should decrease above the Alfvén critical point $r \simeq 10 R_\odot$ according to turbulence models (Cranmer & van Ballegooijen 2012; Perez & Chandran 2013). As a consequence, the parameter $\epsilon = \delta u_0/\sqrt{2} V_\perp$ is expected to decrease with increasing heliocentric distance r, where its highest value is $\epsilon \simeq 0.9$ at $r = 10 R_\odot$ and its lowest value is about 0.03 near 1 au.

Assuming a spectral index $\alpha = 5/3$, we can construct the function $f_\epsilon(\alpha, x)$ versus x for representative values $\epsilon \simeq 0.03$ near 1 au and 0.9 near *PSP* perihelion (left panel of Figure 1). It can be seen that $f_\epsilon(\alpha, x)$ is relatively narrow around $x \simeq 1$ for the small value of ϵ, while for $\epsilon \simeq 0.9$ significant broadening occurs for $f_\epsilon(\alpha, x)$ around its peak value, which is close but not equal to one. Therefore, we anticipate that $f_\epsilon(\alpha, x)$ will be much broader near the Alfvén critical point than around 1 au. The right panel of Figure 1 shows a hypothetical power-law spectrum (on the left vertical axis) versus $k_\perp/k_0$ spanning two decades, where k_0 is some characteristic wavenumber. Just below the power-law spectrum, the function $f_\epsilon(\alpha, \omega/k_\perp V_\perp)$ is shown (on the right vertical axis) versus $k_\perp/k_0$ for a selected frequency $\omega = 5 k_0 V_\perp$. The two plots corresponding to the same values of ϵ in the left panel show the contrast in the interpretation of the same power law at a given frequency. The vertical bars indicate the range of wavenumbers that contribute to about 90% of the energy. Near Earth's orbit, most of the energy at each frequency is sharply localized around $\omega \simeq k_\perp V_\perp$, whereas the same amount of energy is spread over a wider range of wavenumbers near the Sun.

5. Conclusions

In this Letter we introduced an analytical model for the two-time energy spectrum given by Equation (10) based on two minimal assumptions that apply to a wide range of solar wind conditions: (1) the temporal decorrelation for the Eulerian fields $\boldsymbol{z}^{\pm}(\boldsymbol{x}, t)$ is a consequence of random sweeping of the small-scale eddies by large-scale ones; and (2) the turbulence is strongly magnetized $\delta v_{\rm A}' \ll v_{\rm A}$. It then follows that the decorrelation in time of the turbulent eddies is controlled by random sweeping due to large-scale fluid velocities and by pure Alfvénic propagation. This seems to be consistent with earlier obtained results using numerical simulations of strongly MHD turbulence (Lugones et al. 2016, Bourouaine & Perez 2018).

The analytical model for the two-time energy spectrum was used to develop a methodology to connect time signals to the spatial properties of the underlying solar wind turbulence under typical conditions that *PSP* might encounter. The proposed method solely depends on the two measurable parameters, ϵ and α, from where one can determine $x_{\min}$ and $x_{\max}$ to estimate the broadening in $k_\perp$ as $\Delta k_\perp = [k_{\min}, k_{\max}]$ for a given frequency ω where $k_{\min} = \omega/x_{\max} V_\perp$ and $k_{\max} = \omega/x_{\min} V_\perp$. For example, the right panel of Figure 1 shows a hypothetical Kolmogorov power-law spectrum $E(k_\perp) \simeq k_\perp^{-5/3}$ together with the range of wavenumbers that contribute to 90% of the energy at a given frequency for two different values of ϵ. These parameters were chosen to represent typical values expected near *PSP* perihelion and near 1 au.

The model we proposed for the two-time energy spectrum and the resulting methodology differs from previous works in that it requires no assumptions about the turbulence dynamics and is based on just two parameters that can be easily calculated from data. A key physical difference of our model with Narita (2017) is that the spectral broadening is the same for both Elsässer fluctuations, as it only results from hydrodynamic sweeping. The random variation of the magnetic field associated with the large-scale eddies only plays a role in defining the direction of the local magnetic field along which small eddies propagate, but it does not enter in the sweeping to first order in $\delta v_A/v_A$. The proposed methodology also applies to any spacecraft, including those flying in the magnetosheath (like the Magnetospheric Multiscale Mission). Although our model was obtained for Alfvénic fluctuations, we conjecture that the KSH may in principle be extended to turbulence in kinetic scales whenever large-scale sweeping dominates any kinetic decorrelation timescales. More intuitively, the KSH can be seen as the TH applied to an ensemble of systems in which frozen small-scale structures are swept by a constant but random flow. However, because this regime requires a kinetic description of the turbulence dynamics, it requires further investigation.

This work was supported by grant NNX16AH92G from NASA's Living with a Star Program. High-performance-computing resources were provided by the Argonne Leadership Computing Facility (ALCF) at Argonne National Laboratory, which is supported by the Office of Science of the U.S. Department of Energy under contract DE-AC02-06CH11357. The ALCF resources were granted under the INCITE program between 2012 and 2014. High-performance computing resources were also provided by the Texas Advanced Computing Center (TACC) at The University of Texas at Austin, under the NSF-XSEDE Project TG-ATM100031.

ORCID iDs

Jean C. Perez https://orcid.org/0000-0002-8841-6443

References

Alexandrova, O., Saur, J., Lacombe, C., et al. 2010, in AIP Conf. Proc. 1216, 12th International Solar Wind Conference, ed. M. Maksimovic et al. (Melville, NY: AIP), 144
Bourouaine, S., Alexandrova, O., Marsch, E., & Maksimovic, M. 2012, ApJ, 749, 102
Bourouaine, S., & Chandran, B. D. G. 2013, ApJ, 774, 96
Bourouaine, S., & Perez, J. C. 2018, ApJL, 858, L20
Chen, C. H. K., Leung, L., Boldyrev, S., Maruca, B. A., & Bale, S. D. 2014, GeoRL, 41, 8081
Cranmer, S. R., & van Ballegooijen, A. A. 2012, ApJ, 754, 92
Fox, N. J., Velli, M. C., Bale, S. D., et al. 2016, SSRv, 204, 7
Horbury, T. S., Forman, M., & Oughton, S. 2008, PhRvL, 101, 175005
Klein, K. G., Howes, G. G., & TenBarge, J. M. 2014, ApJL, 790, L20
Klein, K. G., Perez, J. C., Verscharen, D., Mallet, A., & Chandran, B. D. G. 2015, ApJL, 801, L18
Kraichnan, R. H. 1964, PhFl, 7, 1723
Lugones, R., Dmitruk, P., Mininni, P. D., Wan, M., & Matthaeus, W. H. 2016, PhPl, 23, 112304
Matthaeus, W. H., Dasso, S., Weygand, J. M., Kivelson, M. G., & Osman, K. T. 2010, ApJL, 721, L10
Matthaeus, W. H., Weygand, J. M., & Dasso, S. 2016, PhRvL, 116, 245101
Narita, Y. 2017, NPGeo, 24, 203
Narita, Y., Glassmeier, K.-H., Motschmann, U., & Wilczek, M. 2013, EP&S, 65, e5
Perez, J. C., & Chandran, B. D. G. 2013, ApJ, 776, 124
Servidio, S., Carbone, V., Dmitruk, P., & Matthaeus, W. H. 2011, EL, 96, 55003
Taylor, G. I. 1938, RSPSA, 164, 476
Weygand, J. M., Matthaeus, W. H., Kivelson, M. G., & Dasso, S. 2013, JGRA, 118, 3995